Ceramics International 51 (2025) 53426–53431

Contents lists available at ScienceDirect

Ceramics International

journal homepage: www.elsevier.com/locate/ceramint

# Spectroscopic study of the $Tb^{3+}$→$Eu^{3+}$ energy transfer process in $TbAl_3(BO_3)_4$ doped with 1 % mol of $Eu^{3+}$ in the 12–310 K temperature range

Leonardo Ceccon [a], Silvia Ruggieri [a], Marco Bettinelli [a], Luís D. Carlos [b], Carlos D.S. Brites [b], Albano N. Carneiro Neto [b], Fabio Piccinelli [a,*]

[a] Luminescent Materials Laboratory, Dipartimento di Biotecnologie, University of Verona and, INSTM, UdR Verona, Strada Le Grazie 15, 37134, Verona, Italy
[b] Phantom-g, CICECO – Aveiro Institute of Materials, Department of Physics, University of Aveiro, 3810–193, Aveiro, Portugal

ARTICLE INFO

Handling editor: P. Vincenzini

ABSTRACT

The $Tb^{3+}$-to-$Eu^{3+}$ non-radiative energy transfer was studied through temperature-dependent luminescence spectroscopy (12−310 K), in $TbAl_3(BO_3)_4$ crystals doped with 1 % mol $Eu^{3+}$ grown in a $K_2SO_4$-$MoO_3$ flux. Excitation and emission spectra were recorded and analyzed, along with the luminescence decay curves of the $Tb^{3+}$ emitting level ($^5D_4$). In the temperature range of 110–310 K, the decay curves were fitted using an adaptation of the Parent et al. model [20], where the $Tb^{3+}$-to-$Eu^{3+}$ energy transfer process is described by the *W* parameter, representing the energy migration-assisted transfer. *W* (and thus the $Tb^{3+}$-to-$Eu^{3+}$ transfer probability) decreases as temperature drops, reaching a plateau around 100 K. Below this temperature, the transfer probability remains relatively unaffected by further temperature reductions, likely due to the influence of non-regular $Tb^{3+}$ ions on the excited state dynamics of the $^5D_4$ level.

## 1. Introduction

$Tb^{3+}$→$Eu^{3+}$ energy transfer process has been broadly investigated and exploited in inorganic-based materials [1–3] to design efficient luminescent compounds emitting in the visible spectral region for the development of optical devices based on innovative phosphors. In this context, efficient red-emitting phosphors can be obtained by exploiting the sensitization of the visible $Eu^{3+}$ luminescence (located in the red spectral region) by $Tb^{3+}$ ions. Representative compounds belonging to this class are materials doped with a small molar percentage of $Eu^{3+}$ (typically 1–10 %) such as cubic $Sr_3Tb(PO_4)_3$ [4], tetragonal $TbPO_4$ [5], and orthorhombic $Ca_3Tb_2Si_3O_{12}$ [6]. In some cases, the $Tb^{3+}$→$Eu^{3+}$ energy transfer efficiency cannot be optimal, allowing the ratio between the $Tb^{3+}$ emission (in the green) and the red emission of $Eu^{3+}$ to be adjusted by varying the concentration of the latter dopant ion. This is the typical case of rhombohedral $Ca_9Tb(PO_4)_7$ [7] and trigonal $TbAl_3(BO_3)_4$ [8,9] hosts doped with $Eu^{3+}$.

On the other hand, the spectroscopic properties of undoped and doped $TbAl_3(BO_3)_4$ have been extensively studied [10–15]. This borate compound crystallizes in a trigonal huntite-type structure (space group No. 155, *R32*) [16] and the point symmetry of the single site accommodating $Tb^{3+}$ is 32 ($D_3$ in the Schönflies notation) and it is surrounded by a trigonal prism of six crystallographically equivalent oxygen atoms (coordination number of 6). The shortest $Tb^{3+}$–$Tb^{3+}$ distance is relatively long (5.889 Å), since the two adjacent $Tb^{3+}$ ions are bridged by one $BO_3^{3-}$ anion. In nominally undoped single crystals grown in a $K_2SO_4$-$MoO_3$ flux, the migration of the excitation energy among $Tb^{3+}$ ions to $Mo^{3+}$ impurities (quenching centres) is governed by electric multipole interactions, as the exchange mechanism requiring shorter $Ln^{3+}$-$Ln^{3+}$ distances can be ruled out. Furthermore, as demonstrated by Kellendonk and Blasse [17] above 60 K, the diffusion-limited $Tb^{3+}$→$Mo^{3+}$ energy transfer is the dominant process. Below this temperature, the dynamic of this energy transfer process is affected by the presence of $Tb^{3+}$ ions in non-regular crystal sites. It has been demonstrated in the literature that in borates with huntite structure few percent of $Ln^{3+}$ ions were incorporated on $Al^{3+}$ [18] and on interstitial sites having molybdenum or bismuth impurity in the nearest surrounding [19]. Therefore, it is reasonable to assume that in the case of $TbAl_3(BO_3)_4$ crystals, some $Tb^{3+}$ ions are also incorporated on these sites.

* Corresponding author.
*E-mail address:* fabio.piccinelli@univr.it (F. Piccinelli).

https://doi.org/10.1016/j.ceramint.2025.09.090
Received 22 July 2025; Received in revised form 3 September 2025; Accepted 4 September 2025
Available online 5 September 2025

In this contribution, we continue our ongoing study of the $Tb^{3+}$→$Eu^{3+}$ energy transfer in $TbAl_3(BO_3)_4$. In the previous papers, the process was investigated at room temperature as a function of the concentration of the acceptor ion ($Eu^{3+}$) [8,9]. Upon fitting the $^5D_4$ decay curve of $Tb^{3+}$ at room temperature, using an adaptation of the Parent et al. [20], we demonstrated that in this material two processes are dominant: *i)* direct energy transfer from $Tb^{3+}$ to quenching centres (crystal defects or $Mo^{3+}$ ions), and *ii)* $Tb^{3+}$→$Eu^{3+}$ energy transfer assisted by energy migration among $Tb^{3+}$ ions of the sublattice. The latter is increasingly important as the $Eu^{3+}$ concentration rises.

In this context, in which is reasonable to assume that the rate of the energy migration among $Tb^{3+}$ ions is higher than the rate of $Tb^{3+}$→$Eu^{3+}$ energy transfer, as already found in many other systems [3,21], we studied the spectroscopic properties of $TbAl_3(BO_3)_4$ doped with $Eu^{3+}$ as a function of the temperature in the 12–310 K range. In this interval, excitation, emission spectra, and decay curves of $^5D_4$ have been recorded and analyzed while keeping constant the $Eu^{3+}$ concentration at 1 % mol, to provide a clear picture about the impact of the temperature on the dynamics of the $Tb^{3+}$→$Eu^{3+}$ energy transfer process. The temperature-dependent changes in the $Tb^{3+}$/$Eu^{3+}$ emission intensity ratio and the $^5D_4$ decay dynamics can be further exploited for luminescence thermometry, using either intensity- or lifetime-based readouts. This approach aligns with previous studies on mixed $Tb^{3+}$/$Eu^{3+}$ luminescent thermometers, which have established the $Tb^{3+}$→$Eu^{3+}$ energy transfer mechanism as a reliable method for engineering optical probes with tunable thermal sensitivity [22–24].

## 2. Experimental

Samples with $TbAl_3(BO_3)_4$:1 % mol $Eu^{3+}$ ($Tb_{0.99}Eu_{0.01}Al_3(BO_3)_4$) stoichiometry were obtained as single crystals following the protocol reported in the literature [8]. In detail, Stoichiometric amounts of $Al_2O_3$ and $Tb_4O_7$, $Eu_2O_3$ corresponding to 1 % mol of $Eu^{3+}$ ion and 30 % molar excess of $B_2O_3$ were mixed with the flux [a mixture of $MoO_3$ and $K_2SO_4$ (3:1 M ratio)] and kept in a platinum crucible with platinum lid. The mixture was heated to 1200 °C in 5 h and then maintained at this temperature for 5 h. The system was cooled to 1120 °C in 5 h. Finally, the sample was slowly cooled down to 885 °C with a rate of 1.2 °C/h and then quickly to room temperature. Upon removing the flux by boiling the raw materials in concentrated solution of NaOH (8 M), transparent crystals were obtained.

X-ray diffraction (XRD) pattern was measured with a Thermo ARL X'TRA powder diffractometer, operating in the Bragg-Brentano geometry and equipped with a Cu-anode X-ray source ($K_\alpha$, $\lambda = 1.5418$ Å), using a Peltier Si(Li) cooled solid state detector. The patterns were collected with a scan rate of 0.04°/s in the 10°–90° $2\theta$ range. Few crystals of the compounds were ground in a mortar and then put in the sample holder for the data collection.

The temperature-dependent decay curve, emission, and excitation spectra were recorded using a modular double grating excitation spectrofluorometer featuring a TRIAX 320 emission monochromator (Fluorolog-3, Horiba Scientific) coupled with a R298 Hamamatsu photomultiplier and a H9170 Hamamatsu photomultiplier, employing a front face acquisition mode. The excitation source utilized was a Xe lamp. The temperature was adjusted by a He-closed cycle cryostat coupled to a vacuum system ($4 \times 10^{-4}$ Pa), and an autotuning temperature controller (Lakeshore 330, Lakeshore) equipped with a resistance heater. The temperature was measured by a silicon diode cryogenic sensor (DT-470-SD, Lakeshore) with an accuracy of ±0.5 K (12–30 K), ±0.25 K (30–60 K), and ±0.15 K (60–385 K). All the decay curves, emission, and excitation spectra were recorded only after the temperature indicated in the temperature controller stabilized, ensuring both sample thermalization and a constant temperature throughout the measurement.

## 3. Results and discussion

In Fig. 1, the X-ray diffraction powder pattern of ground crystal of $TbAl_3(BO_3)_4$:1 % mol $Eu^{3+}$ is reported. As expected, a pure trigonal huntite-type structure (space group No. 155, *R32*) was obtained.

In Fig. 2, the excitation spectra of the $Eu^{3+}$ emission are reported upon monitoring the $^5D_0$→$^7F_4$ emission at five different temperatures (i.e., 12, 85, 160, 235, and 310 K) for the sample $TbAl_3(BO_3)_4$:1 % mol $Eu^{3+}$.

In these spectra, we observe the presence of the excitation peaks related to *f-f* transitions of both $Tb^{3+}$ and $Eu^{3+}$ ions, as labeled in Fig. 2. It is interesting to note that, upon normalization of the spectra to the $^7F_0$→$^5D_2$ excitation peak of $Eu^{3+}$, the intensity of the excitation peaks of $Tb^{3+}$ does not change significantly with the temperature in the 12–160 K temperature range. On the contrary, upon increasing the temperature to 235 and 310 K, a gradual increase of the intensity of these peaks is recorded; this is compatible with an increase of the $Tb^{3+}$→$Eu^{3+}$ energy transfer efficiency. Also, the $^7F_1$→$^5D_0$ excitation peak of the $Eu^{3+}$ ion gains intensity at these temperatures.

In Fig. 3a, the $^5D_4$ decay curves of $Tb^{3+}$ luminescence in $TbAl_3(BO_3)_4$:1 % mol $Eu^{3+}$ are presented as a function of the temperature (12–310 K).

We observe some differences among the curves as the temperature changes. In particular, as temperature increases, the decay of luminescence intensity becomes faster. We were able to fit the decay curves in the 110–310 K temperature range using a model adapted from that proposed by Parent et al., as reported in our previous paper [9] (Fig. 3b). The mathematical expression of the fitting equation, in the case of electric dipole-electric dipole interaction, is:

$$I(t) = I(0)exp\left[-\frac{t}{\tau_{5D4}} - Q_{5D4}\left(\frac{t}{\tau_{5D4}}\right)^{\frac{1}{2}} - Wt\right] \quad (1)$$

where $Q_{5D4}$ refers to the direct energy transfer from $Tb^{3+}$ to quenching centres without energy migration within the $Tb^{3+}$ subset of ions, while $W$ represents the influence of the energy migration function in the $Tb^{3+}$ subset on the $Tb^{3+}$→$Eu^{3+}$ energy transfer. It is useful to note that $W$ is proportional to the product of the donor ($Tb^{3+}$) and acceptor ($Eu^{3+}$) concentrations (here constants) and it is related to $C_{DD(Tb\text{-}Tb)}$ and $C_{DA}$

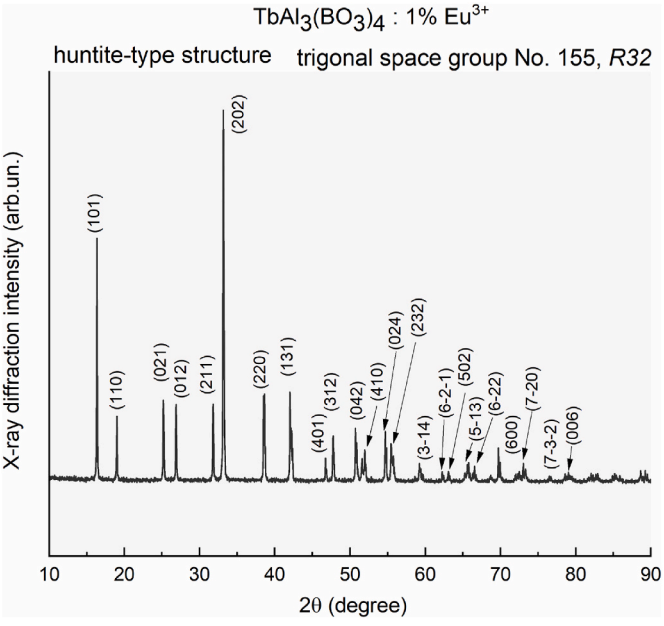


**Fig. 1.** X-ray diffraction powder pattern of the $TbAl_3(BO_3)_4$:1 % mol $Eu^{3+}$ under investigation. The Miller indexes of the main diffraction peaks of the huntite-type structure are reported.

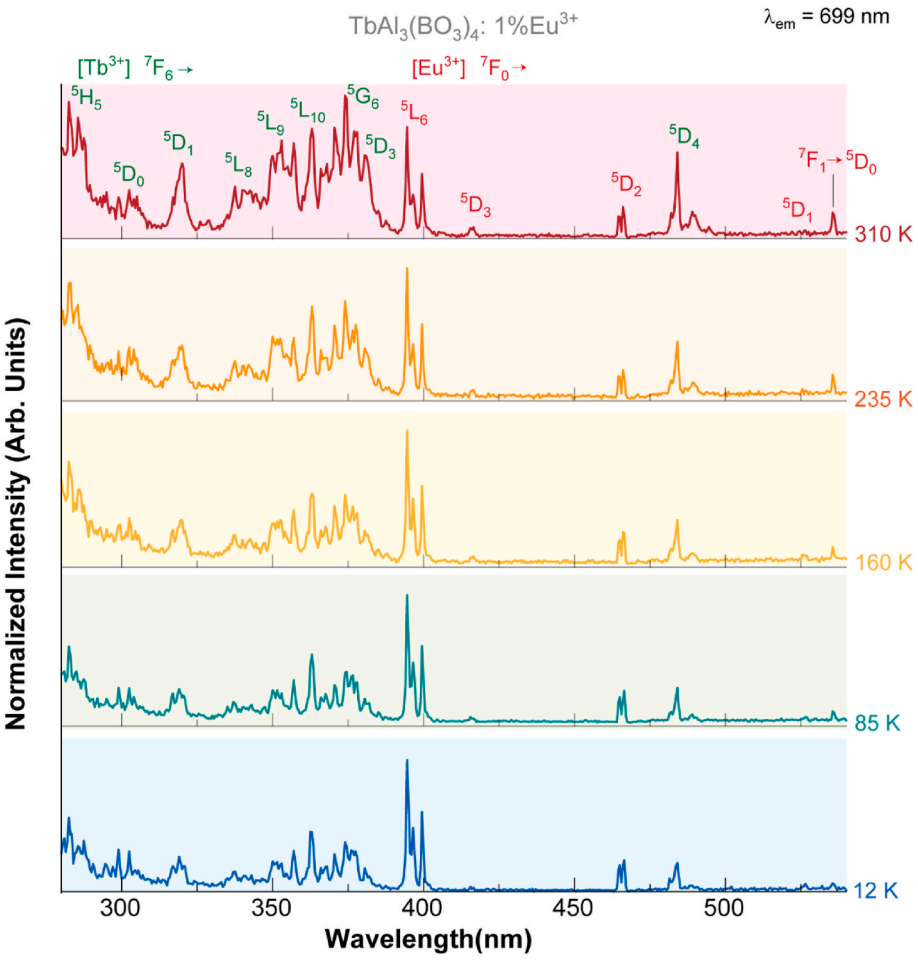


**Fig. 2.** Normalized excitation spectra of the $Eu^{3+}$ emission at 699 nm recorded at different temperatures: in the 12–310 K range. The spectra are normalized to the area of the $^7F_0 \rightarrow {}^5D_2$ excitation peak of $Eu^{3+}$.

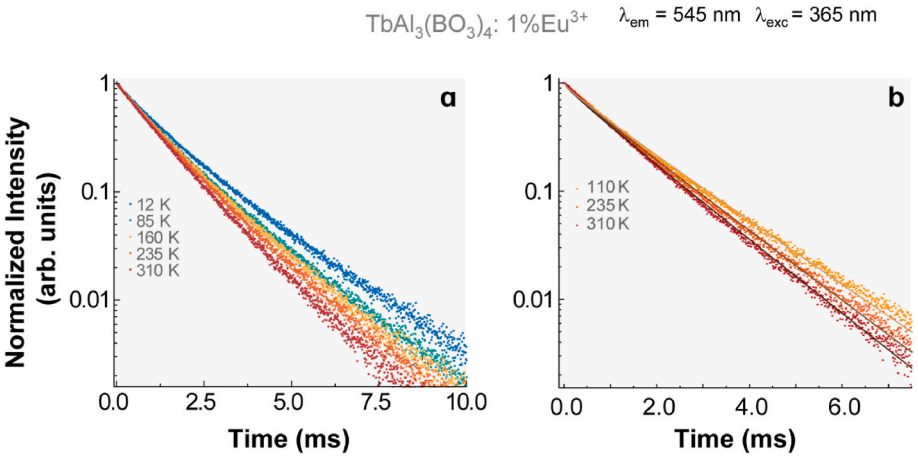


**Fig. 3.** $^5D_4$ $Tb^{3+}$ decay curves at different temperatures, upon excitation at 365 nm of $TbAl_3(BO_3)_4$:1 % mol $Eu^{3+}$; in the 12–310 K range (a) and magnification of the curves at 110–310 K to better appreciate the graphical fitting of equation (1) (b).

$_{(TbEu)}$, the microparameters for $Tb^{3+} \rightarrow Tb^{3+}$ energy migration and $Tb^{3+} \rightarrow Eu^{3+}$ energy transfer, respectively. Considering a dipole-dipole interaction between donor ($Tb^{3+}$ ion) and acceptors (quenching centres and $Eu^{3+}$), the intrinsic decay constant of $Tb^{3+}$ ($\tau_{5D4}$) was fixed at 1.9 ms [9] and the fitted $Q_{5D4}$ and $W$ values are reported in Table 1.

As the temperature decreases, both the $Q_{5D4}$ and $W$ values moderately decrease, even though the change in $Q_{5D4}$ is almost negligible. The change of W with the temperature is depicted in Fig. 4a.

$W$ value decreases upon decreasing the temperature down to 160 K, then it seems to approach a constant value. A similar trend is observed when the area of the excitation peaks in the 330–390 nm range reported in Fig. 2 is plotted as a function of the temperature (Fig. 4b). This wavelength region is dominated by the excitation peaks of $Tb^{3+}$.

The decay curves at temperatures lower than 85 K cannot be fitted

**Table 1**
Fitted values of $Q_{5D4}$ and $W$ in eq. (1) at different temperatures for $TbAl_3(BO_3)_4$:1 % mol $Eu^{3+}$.

| Temperature (K) | Fitted value of $Q_{5D4}$ | Fitted value of $W$ ($ms^{-1}$) |
|---|---|---|
| 110 | 0.20(1) | 0.11(1) |
| 160 | 0.21(1) | 0.12(1) |
| 235 | 0.22(1) | 0.17(1) |
| 310 | 0.24(1) | 0.22(1) |

satisfactorily by using equation (1). In Fig. 5, two representative emission spectra of $TbAl_3(BO_3)_4$:1 % mol $Eu^{3+}$ upon excitation of $Tb^{3+}$ ions at 374 nm, at 60 and 310 K, are reported. As expected, the emission intensity of $Eu^{3+}$ (*i.e.* $^5D_0 \rightarrow {}^7F_1$, $^5D_0 \rightarrow {}^7F_2$, $^5D_0 \rightarrow {}^7F_4$) compared to the emission of $Tb^{3+}$ is higher at 310 than at 60 K.

Finally, upon direct excitation of $Eu^{3+}$ ions at 394 nm, only the typical *f-f* emission spectrum from the $^5D_0$ level of this ion is observed (Fig. 6). In these conditions, since no emission peaks belonging to the *f-f* transitions of $Tb^{3+}$ are detectable, the occurrence of $Eu^{3+} \rightarrow Tb^{3+}$ back energy transfer process can be ruled out.

In the trigonal huntite-type structure, the $Eu^{3+}$ ion in $D_3$ symmetry exhibits two crystal field components for both $^5D_0 \rightarrow {}^7F_1$ and $^5D_0 \rightarrow {}^7F_2$ transitions and four components for both $^5D_0 \rightarrow {}^7F_3$ and $^5D_0 \rightarrow {}^7F_4$ [18, 25]. Our spectrum agrees well with this picture, even though a very low intensity of the $^5D_0 \rightarrow {}^7F_3$ peaks and one Stark component of the $^5D_0 \rightarrow {}^7F_4$ transition is observed.

As already stated, the gradual increase of the $Tb^{3+}$ excitation peaks observed in Fig. 1 upon increasing the temperature above 160 K is related to the increase of the $Tb^{3+} \rightarrow Eu^{3+}$ energy transfer efficiency. Upon increasing the temperature, the thermal population of the $^7F_1$ level of $Eu^{3+}$ is increased, as confirmed by the growth of the intensity of the $^7F_1 \rightarrow {}^5D_0$ excitation peak of the $Eu^{3+}$ with the temperature above 160 K (Fig. 2). Therefore, also the involvement in the energy transfer process of $^7F_1$ is promoted at these temperatures. In this context, it is well known that an efficient energy transfer from $Tb^{3+}$ to $Eu^{3+}$ can involve the almost resonant $^5D_4 \rightarrow {}^7F_5$ (for $Tb^{3+}$) and $^7F_1 \rightarrow {}^5D_1$ (for $Eu^{3+}$) transitions, characterized by an energy mismatch of only 259 $cm^{-1}$. As an example, this channel is mainly responsible for the energy transfer from $Tb^{3+}$ to $Eu^{3+}$ in cubic $A_3Tb_{0.90}Eu_{0.10}(PO_4)_3$ (A = Sr, Ba) compounds [21]. At low temperature, this energy transfer channel is no longer so efficient since the main $Eu^{3+}$ level involved in the energy transfer would be the $^7F_0$. Therefore, transitions such as $^7F_0 \rightarrow {}^5D_0$ and $^7F_0 \rightarrow {}^5D_1$ could participate in the energy transfer process. However, the former electronic transition is highly forbidden, and its intensity is usually very low [26]. On the other hand, the latter transition is purely magnetic dipole allowed, and it is well known that couplings formally involving magnetic dipole transitions give rise to low energy transfer probabilities [27].

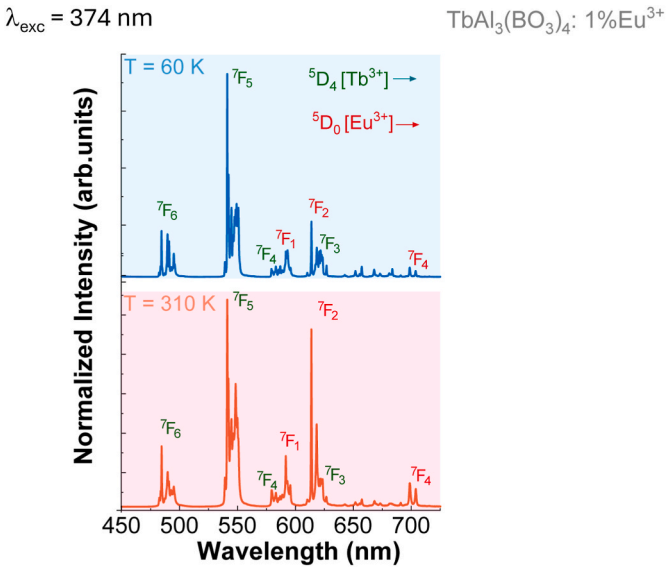


**Fig. 5.** Emission spectra at 60 K and 310 K of $TbAl_3(BO_3)_4$:1 % mol $Eu^{3+}$ upon excitation of $Tb^{3+}$ ions at 374 nm. The spectra are normalized to the maximum intensity of the $^5D_4 \rightarrow {}^7F_5$ transition of $Tb^{3+}$.

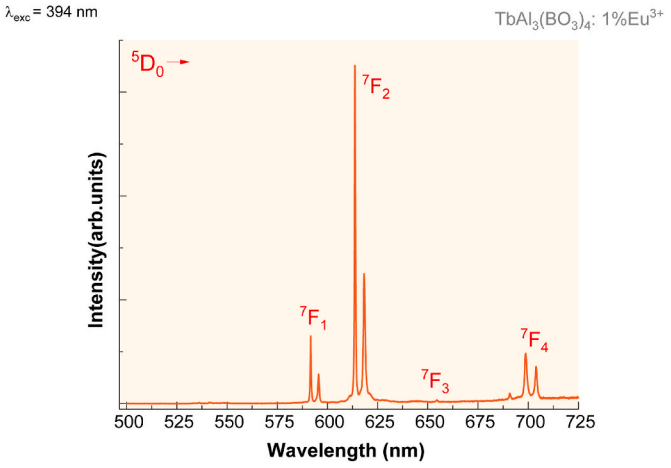


**Fig. 6.** Emission spectrum of $TbAl_3(BO_3)_4$:1 % mol $Eu^{3+}$ at 310 K upon direct excitation of $Eu^{3+}$ ion at 394 nm.

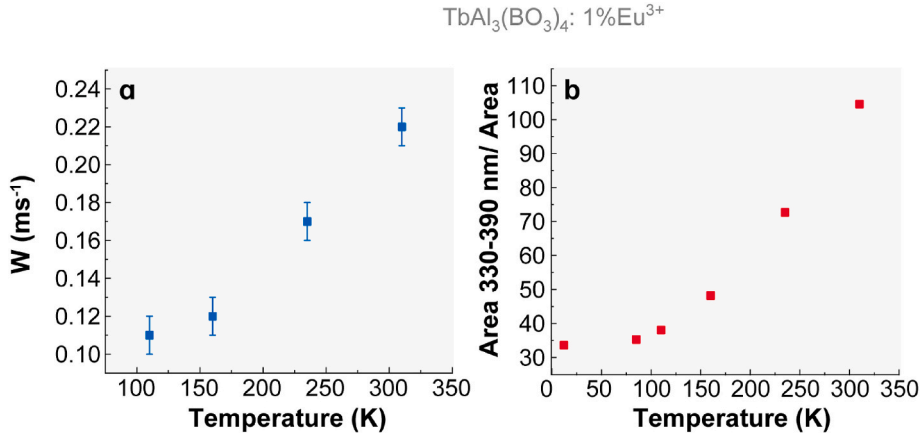


**Fig. 4.** (a) $W$ ($ms^{-1}$) *vs* temperature for $TbAl_3(BO_3)_4$:1 % mol $Eu^{3+}$ and (b) ratio between the area of the $Tb^{3+}$ excitation peaks (in the 330–390 nm range) and the area of the $Eu^{3+}$ $^7F_0$-$^5D_2$ excitation peak, as a function of the temperature.

The similar trend of the plots in Fig. 4 is very interesting and point out that the energy transfer efficiency seems to trace the temperature dependence of the *W* parameter, in turn directly connected to the $Tb^{3+}$→$Eu^{3+}$ energy transfer probability.

The weak but significant change of trend of the $^5D_4$ decay curves observed below 85 K (Fig. 3a) can be reasonably attributed to the presence of the $Tb^{3+}$ traps in non-regular crystal sites, discussed in the introduction, that should affect the dynamics of the $Tb^{3+}$→$Eu^{3+}$ energy transfer. In this context, a different theoretical description is required to fit the decay curves at low temperatures. This lies beyond the scope of the present investigation.

## 4. Conclusions

In this paper, the results of a spectroscopic study on $TbAl_3(BO_3)_4$:1 % mol $Eu^{3+}$ sample as a function of temperature have been presented. We demonstrate that the efficiency of the $Tb^{3+}$→$Eu^{3+}$ energy transfer mechanism increases gradually upon increasing the temperature above 100 K, when the thermal population of the $^7F_1$ level of $Eu^{3+}$ begins to be non-negligible and therefore the $^5D_4$→$^7F_5$ and $^7F_1$→$^5D_1$ transitions of $Tb^{3+}$ and $Eu^{3+}$, respectively, can be involved in the energy transfer process. In the 100–310 K temperature range, the fitting of the $^5D_4$ decay curves at different temperatures using an adaptation of the Parent et al. model [20], supports this conclusion: the refined values of the *W* parameter, closely linked to the $Tb^{3+}$→$Eu^{3+}$ energy transfer probability, increase with the temperature. On the other hand, the *W* parameter no longer seems to vary with temperature below 150 K and takes a minimum value of 0.11 $ms^{-1}$. Accordingly, inspection of the excitation spectra in the 12–100 K temperature range reveals that the $Tb^{3+}$→$Eu^{3+}$ energy transfer efficiency does not change significantly. However, below 100 K, a different mathematical model is required to properly fit the $^5D_4$ decay curves. At these temperatures, the dynamics of the energy transfer process possibly changes because $Tb^{3+}$ ions in non-regular crystal sites may affect the $Tb^{3+}$→$Eu^{3+}$ energy transfer dynamics. For potential applications in luminescence thermometry, this material offers two distinct temperature-sensing mechanisms. The temperature-dependent $^5D_4$ lifetime can be used for sensing across the entire 12–310 K range. In contrast, the relative emission intensities of $Tb^{3+}$ and $Eu^{3+}$ ions are only sensitive to temperature changes above 100 K. This highlights the ability to use either or both methods, depending on the specific temperature range of interest.

## CRediT authorship contribution statement

**Leonardo Ceccon:** Investigation, Formal analysis. **Silvia Ruggieri:** Data curation. **Marco Bettinelli:** Conceptualization. **Luís D. Carlos:** Supervision. **Carlos D.S. Brites:** Validation. **Albano N. Carneiro Neto:** Data curation. **Fabio Piccinelli:** Writing – original draft, Supervision.

## Declaration of competing interest

The authors declare that they have no known competing financial interests or personal relationships that could have appeared to influence the work reported in this paper.

## Acknowledgments

The authors gratefully thank Inocencio R. Martin from the Department of Physics, Instituto de Materiales y Nanotecnología (IMN), University of La Laguna, S/C de Tenerife, Spain, for the useful discussion on the kinetic model adopted in this contribution, and Erica Viviani from the University of Verona for expert technical assistance. Authors from the University of Verona gratefully thank the Facility "Centro Piattaforme Tecnologiche" (CPT) for access to the Fluorolog 3 (Horiba-Jobin Yvon) spectrofluorometer. This work was partially developed within the scope of the projects CICECO - Aveiro Institute of Materials, UIDB/50011/2020 (DOI:10.54499/UIDB/50011/2020), UIDP/50011/2020 (DOI: 10.54499/UIDP/50011/2020) and LA/P/0006/2020 (DOI:10.54499/LA/P/0006/2020) financed by Portuguese funds through the FCT/MEC (PIDDAC), and when appropriate, cofinanced by FEDER under the PT2020 Partnership through European Regional Development Fund (ERDF) in the frame of Operational Competitiveness and Internationalization Programme (POCI). LC thanks Fernando Maturi and Julio Corredoira-Vázquez (University of Aveiro) for the help with the temperature-dependent luminescence measurements.

## References

[1] W.W. Holloway Jr., J.M. Kestigian, R. Newman, Direct evidence for energy transfer between rare earth ions in terbium-europium tungstates, Phys. Rev. Lett. 11 (1963) 458–460, https://doi.org/10.1103/PhysRevLett.11.458.

[2] M. Bettinelli, C.D. Flint, Non-resonant energy transfer between $Tb^{3+}$ and $Eu^{3+}$ in the cubic hexachloroelpasolite crystals $Cs_2NaTb_{1-x}Eu_xCl_6$ (x=0.01-0.15), J. Phys. Condens. Matter 2 (1990) 8417–8426, https://doi.org/10.1088/0953-8984/2/42/018.

[3] I. Carrasco, F. Piccinelli, M. Bettinelli, Luminescence of Tb-based materials doped with $Eu^{3+}$: case studies for energy transfer processes, J. Lumin. 189 (2017) 71–77, https://doi.org/10.1016/j.jlumin.2016.06.065.

[4] M. Bettinelli, A. Speghini, F. Piccinelli, J. Ueda, S. Tanabe, Energy transfer processes in $Sr_3Tb_{0.90}Eu_{0.10}(PO_4)_3$, Opt. Mater. 33 (2010) 119–122, https://doi.org/10.1016/j.optmat.2010.07.008.

[5] I. Carrasco, F. Piccinelli, I. Romet, V. Nagirnyi, M. Bettinelli, Competition between energy transfer and energy migration processes in neat and $Eu^{3+}$-doped $TbPO_4$, J. Phys. Chem. C 122 (2018) 6858–6864, https://doi.org/10.1021/acs.jpcc.8b01374.

[6] I. Carrasco, K. Bartosiewicz, M. Nikl, F. Piccinelli, M. Bettinelli, Energy transfer processes in $Ca_3Tb_{2-x}Eu_xSi_3O_{12}$ (x = 0–2), Opt. Mater. 48 (2015) 252, https://doi.org/10.1016/j.optmat.2015.08.009.

[7] I. Carrasco, F. Piccinelli, M. Bettinelli, Optical spectroscopy of $Ca_9Tb_{1-x}Eu_x(PO_4)_7$ (x = 0, 0.1, 1): weak donor energy migration in the whitlockite structure, J. Phys. Chem. C 121 (2017) 16943–16950, https://doi.org/10.1021/acs.jpcc.7b05920.

[8] S. Ruggieri, L. Ceccon, M. Bettinelli, F. Piccinelli, Excited state dynamics of undoped and $Eu^{3+}$-doped $TbAl_3(BO_3)_4$ crystals, ECS J. Solid State Sci. Technol. 12 (2023) 066005, https://doi.org/10.1149/2162-8777/acde0d.

[9] L. Ceccon, S. Ruggieri, M. Bettinelli, I.R. Martin, F. Piccinelli, $Tb^{3+}$→$Eu^{3+}$ energy transfer processes in crystals of $TbAl_3(BO_3)_4$ doped with $Eu^{3+}$, Ceram. Int. 51 (2025) 16471–16474, https://doi.org/10.1016/j.ceramint.2024.09.285.

[10] A.V. Peschanskii, A. Yu Glamazda, I.A. Gudim, Spectroscopic study of the $TbAl_3(BO_3)_4$ single crystal: raman and luminescence spectroscopy, Low Temp. Phys. 46 (2020) 1223–1230, https://doi.org/10.1063/10.0002478.

[11] J. Huang, Y. Lin, X. Gong, Y. Huang, Y. Chen, Growth, spectroscopy and $Dy^{3+}$→$Tb^{3+}$ energy transfer of $TbAl_3(BO_3)_4$ and $Dy^{3+}$:$TbAl_3(BO_3)_4$ crystals, Opt. Mater. 150 (2024) 115287, https://doi.org/10.1016/j.optmat.2024.115287.

[12] I. Couwenberg, K. Binnemans, H. De Leebeeck, C. Gorller-Walrand, Spectroscopic properties of the trivalent terbium ion in the huntite matrix $TbAl_3(BO_3)_4$, J. Alloys Compd. 274 (1998) 157–163, https://doi.org/10.1016/S0925-8388(98)00549-0.

[13] C. Gorller-Walrand, P. Vandevelde, I. Hendrickx, P. Porcher, J.C. Krupa, A spectroscopic study of the $TbAl_3(BO_3)_4$ crystal, Inorg. Chim. Acta. 139 (1987) 277–279, https://doi.org/10.1016/S0020-1693(00)84095-5.

[14] J. Lu, C. Fu, J. Chen, Structure, growth, and optical properties of $TbAl_3(BO_3)_4$ single crystal, Appl. Opt. 50 (2011) 116–119, https://doi.org/10.1364/ao.50.000116.

[15] S. Colak, W.K. Zwicker, Transition rates of $Tb^{3+}$ in $TbP_5O_{14}$, $TbLiP_4O_{12}$, and $TbAl_3(BO_3)_4$: an evaluation for laser applications, J. Appl. Phys. 54 (1983) 2156–2166, https://doi.org/10.1063/1.332393.

[16] A.D. Mills, Crystallographic data for new rare Earth borate compounds, $RX_3(BO_3)_4$, Inorg. Chem. 1 (1962) 960. https://pubs.acs.org/doi/10.1021/ic50004a063.

[17] F. Kellendonk, G. Blasse, Luminescence and energy transfer in $TbAl_3B_4O_{12}$, J. Phys. Chem. Solid. 43 (1982) 481, https://doi.org/10.1016/0022-3697(82)90160-3.

[18] F. Kellendonk, G. Blasse, Luminescence and energy transfer in $EuAl_3B_4O_{12}$, J. Chem. Phys. 75 (1981) 561–571, https://doi.org/10.1063/1.442061.

[19] K.N. Boldyrev, M.N. Popova, M. Bettinelli, V.L. Temerov, I.A. Gudim, L. N. Bezmaternykh, P. Loiseau, G. Aka, N.I. Leonyuk, Quality of the rare earth aluminum borate crystals for laser applications, probed by high-resolution spectroscopy of the $Yb^{3+}$ ion, Opt. Mater. 34 (2012) 1885–1889, https://doi.org/10.1016/j.optmat.2012.05.021.

[20] C. Parent, C. Lurin, G. Le Flem, P. Hagenmuller, $Nd^{3+}$ → $Yb^{3+}$ energy transfer in glasses with composition close to $LiLnP_4O_{12}$ metaphosphate (ln = La, Nd, he eYb), J. Lumin. 36 (1986) 49–55, https://doi.org/10.1016/0022-2313(86)90030-X.

[21] A.N. Carneiro Neto, R.T. Moura Jr., A. Shyichuk, V. Paterlini, F. Piccinelli, M. Bettinelli, O.L. Malta, Theoretical and experimental investigation of the $Tb^{3+}$ → $Eu^{3+}$ energy transfer mechanisms in cubic $A_3Tb_{0.90}Eu_{0.10}(PO_4)_3$ (A = Sr, Ba) materials, J. Phys. Chem. C 124 (2020) 10105–10116. https://pubs.acs.org/doi/10.1021/acs.jpcc.0c00759.

[22] C.D.S. Brites, R. Marin, M. Suta, A.N. Carneiro Neto, E. Ximendes, D. Jaque, L. D. Carlos, Spotlight on Luminescence thermometry: basics, challenges, and cutting-edge applications, Adv. Mater. 35 (2023) 2302749, https://doi.org/10.1002/adma.202302749.

[23] V. Trannoy, A.N. Carneiro Neto, C.D.S. Brites, L.D. Carlos, H. Serier-Brault, Engineering of mixed $Eu^{3+}$/$Tb^{3+}$ metal-organic frameworks luminescent thermometers with tunable sensitivity, Adv. Opt. Mater. 9 (2021) 2001938, https://doi.org/10.1002/adom.202001938.

[24] J. Deng, Z. Wang, W. Zhou, M. Yu, J. Min, X. Jiang, Z. Xue, C. Ma, Z. Cheng, G. Luo, Energy transfer of $Tb^{3+}$→$Eu^{3+}$ in $Ca_2Al_2SiO_7$ phosphors with multicolor tunable and optical temperature sensing properties, Ceram. Int. 49 (2023) 14478–14486, https://doi.org/10.1016/j.ceramint.2023.01.036.

[25] C. Görller-Walrand, P. Vandevelde, I. Hendrickx, P. Porcher, J.C. Krupa, G.S. D. King, Spectroscopic study and crystal field analysis of $Eu^{3+}$ in the $YAl_3(BO_3)_4$ huntite matrix, Inorg. Chim. Acta. 143 (1988) 259–270, https://doi.org/10.1016/S0020-1693(00)83699-3.

[26] R.D. Peacock, The intensities of lanthanide f—f transitions, Struct. Bond 22 (1975) 83–122, https://doi.org/10.1007/BFb0116556.

[27] B. Di Bartolo, Energy Transfer Processes in Condensed Matter, NATO Science Series B, Springer, New York, NY, 1985. https://link.springer.com/book/10.1007/978-1-4613-2407-2.